



Contents lists available at ScienceDirect

Journal of Orthopaedic Translation

journal homepage: www.journals.elsevier.com/journal-of-orthopaedic-translation

ORIGINAL ARTICLE

Chondrocyte ferroptosis contribute to the progression of osteoarthritis

Xudong Yao^{a,1}, Kai Sun^{a,1}, Shengnan Yu^b, Jiahui Luo^c, Jiachao Guo^a, Jiamin Lin^a, Genchun Wang^a, Zhou Guo^a, Yaping Ye^a, Fengjing Guo^{a,*}^a Department of Orthopedics, Tongji Hospital, Tongji Medical College, Huazhong University of Science and Technology, Wuhan, Hubei, 430030, PR China^b Department of Oncology, Tongji Hospital, Tongji Medical College, Huazhong University of Science and Technology, Wuhan, Hubei, 430030, PR China^c The Center for Biomedical Research, Ministry of Education and Ministry of Health, Tongji Hospital, Tongji Medical College, Huazhong University of Science and Technology, Wuhan, Hubei, 430030, PR China

ARTICLE INFO

Keywords:

Osteoarthritis
Ferroptosis
Ferrostatin-1
Inflammation
Iron overload

SUMMARY

Background: Osteoarthritis (OA) is a complex process comprised of mechanical load, inflammation, and metabolic factors. It is still unknown that if chondrocytes undergo ferroptosis during OA and if ferroptosis contribute to the progression of OA.**Materials and methods:** In our study, we use Interleukin-1 Beta (IL-1 β) to simulate inflammation and ferric ammonium citrate (FAC) to simulate the iron overload *in vitro*. Also, we used the surgery-induced destabilized medial meniscus (DMM) mouse model to induce OA *in vivo*. We verify ferroptosis by its definition that defined by the Nomenclature Committee on Cell Death with both *in vitro* and *in vivo* model.**Results:** We observed that both IL-1 β and FAC induced reactive oxygen species (ROS), and lipid ROS accumulation and ferroptosis related protein expression changes in chondrocytes. Ferrostatin-1, a ferroptosis specific inhibitor, attenuated the cytotoxicity, ROS and lipid-ROS accumulation and ferroptosis related protein expression changes induced by IL-1 β and FAC and facilitated the activation of Nrf2 antioxidant system. Moreover, erastin, the most classic inducer of ferroptosis, promoted matrix metalloproteinase 13 (MMP13) expression while inhibited type II collagen (collagen II) expression in chondrocytes. At last, we proved that intraarticular injection of ferrostatin-1 rescued the collagen II expression and attenuated the cartilage degradation and OA progression in mice OA model.**Conclusions:** In summary, our study firstly proved that chondrocytes underwent ferroptosis under inflammation and iron overload condition. Induction of ferroptosis caused increased MMP13 expression and decreased collagen II expression in chondrocytes. Furthermore, inhibition of ferroptosis, by intraarticular injection of ferrostatin-1, in our case, seems to be a novel and promising option for the prevention of OA.**The translational potential of this article:** The translation potential of this article is that we first indicated that chondrocyte ferroptosis contribute to the progression of osteoarthritis which provides a novel strategy in the prevention of OA.

Introduction

Osteoarthritis (OA) is the leading cause of disability in seniors and endemic throughout the world. It is estimated that 300 million people worldwide suffered from OA [1]. OA used to be considered as a disease of “wear and tear.” Excessive mechanical load on the joint was thought to lead to the destruction of the articular cartilage. However, researchers

find out that OA is a more complex process composed of inflammation, metabolic factors, and even ABO blood group [2–6]. In addition, OA is regulated by many bioactive molecules such as Wnt and Wnt-related molecule and SOX9 etc [7,8]. Among those contributing factors of OA, inflammation is a major factor associated with both the cartilage loss and symptoms of disease [9]. Inflammatory factors such as interleukin 1 β (IL-1 β) are evaluated in the synovial fluid of both early-stage and

* Corresponding author. Department of Orthopedics, Tongji Hospital, Tongji Medical College, Huazhong University of Science and Technology, No.1095 Jie Fang Avenue, Hankou, Wuhan, 430030, Hubei, PR China.

E-mail addresses: 608983321@qq.com (X. Yao), 1085844308@qq.com (K. Sun), 1334870996@qq.com (S. Yu), 459242047@qq.com (J. Luo), 793527829@qq.com (J. Guo), 1428975034@qq.com (J. Lin), 455703865@qq.com (G. Wang), 1178519539@qq.com (Z. Guo), yyortho@163.com (Y. Ye), guofjdoc@163.com (F. Guo).

¹ These authors contributed equally to this work.

<https://doi.org/10.1016/j.jot.2020.09.006>

Received 14 May 2020; Received in revised form 26 July 2020; Accepted 16 September 2020

2214-031X/© 2020 The Author(s). Published by Elsevier (Singapore) Pte Ltd on behalf of Chinese Speaking Orthopaedic Society. This is an open access article under

the CC BY-NC-ND license (<http://creativecommons.org/licenses/by-nc-nd/4.0/>).

late-stage OA patients [10,11]. Many metabolic factors, such as hyperlipidemia [12,13] and iron overload [14–16] are also closely correlated with OA.

Chondrocytes, as the only cell component of cartilage, maintain the integrity of the extracellular matrix (ECM) by balancing the synthesis and degradation of the ECM [17]. Hence, chondrocyte injuries is a major event during the progression of OA. It's well studied that chondrocyte injuries can be attributed to the cell necrosis, apoptosis and autophagic cell death [18]. In 2012, Dixon et al. firstly reported a new form of regulated cell death that are morphologically, biochemically and genetically different from other forms of regulated cell death and named it ferroptosis [19]. Ferroptosis is an iron-dependent non-apoptotic cell death featured by inactivation of antioxidant enzyme glutathione peroxidase 4 (GPX4) and the accumulation of lipid reactive oxygen species (lipid-ROS). Recent studies have proved that GPX4 is the key regulator of ferroptosis [20]. ACSL4 also is a biomarker and contributor of ferroptosis, although the mechanism is still unclear [21,22]. System Xc⁻ is a cystine/glutamate antiporter. Inhibition of SLC7A11, a subunit that unique to system Xc⁻, causes depletion of intracellular GSH, iron-dependent lipid peroxidation and subsequent ferroptosis [23]. P53, a tumor suppressor that plays critical roles in apoptosis, also plays an important role in ferroptosis by suppressing the expression of SLC7A11 [24]. Recently, the Nomenclature Committee on Cell Death defined ferroptosis as a form of regulated cell death initiated by oxidative perturbations of the intracellular microenvironment that is under constitutive control by GPX4 and can be inhibited by iron chelators and lipophilic antioxidants [25]. So far, ferroptosis is proved to be corrected with many degenerative diseases (such as Alzheimer's disease, Parkinson's diseases and kidney degeneration), carcinogenesis, intracerebral hemorrhage, traumatic brain injury, ischemia-reperfusion injury and stroke [26]. As far as we know, there still no research that explores the roles of ferroptosis in the progression of OA. However, OA does have some features in common with ferroptosis such as abnormal iron metabolism [27–29], lipid peroxidation [30,31] and mitochondrial dysfunction [32,33]. Thus, it's possible that ferroptosis participate in the progression of OA.

In this study, we use Interleukin-1 Beta (IL-1 β) to simulate inflammation and ferric ammonium citrate (FAC) to simulate the iron overload *in vitro*. Also, we used surgery-induced destabilized medial meniscus (DMM) mouse model to induce OA *in vivo*. We aim to explore the roles of ferroptosis in the progression of OA which can provide a novel strategy that prevents the progression of OA by inhibiting chondrocyte ferroptosis.

Materials and methods

Reagents

Ferric ammonium citrate (USA, 1185-57-5) was purchased from Sigma-Aldrich. Recombinant mouse IL-1 β (Minneapolis, USA, # 401-ML) was purchased from R&D systems. Erastin (USA, S7242) and Ferrostatin-1 (USA, S7243) were purchased from Selleck. Reactive Oxygen Species Assay Kit (China, S0033) was purchased from Beyotime. C11 BODIPY Lipid Peroxidation Sensor (USA, D3861) was purchased from ThermoFisher. GPX4 (UK, ab125066, diluted 1:5000) antibody, P53 antibody (UK, ab131442, diluted 1:1000), SLC7A11 antibody (UK, ab175186, diluted 1:5000), ACSL4 (UK, ab155282, diluted 1:10,000) antibody, Collagen II (UK, ab34712, diluted 1:200 for immunohistochemical staining) antibody, Collagen II (UK, ab185430, diluted 1:1000 for western blot) antibody, NQO-1 antibody (UK, ab80588, diluted 1:10,000), and Trx (UK, ab133524, diluted 1:10,000) antibody were purchased from Abcam. Nrf2 antibody (USA, 16396-1-AP, diluted 1:1000), HO-1 antibody (USA, 10701-1-AP, diluted 1:1000), Beta-actin antibody (USA, 66009-1-Ig, diluted 1:1000) and GAPDH antibody (USA, 60004-1-Ig, diluted 1:1000) were purchased from Proteintech.

Isolation and culture of mouse chondrocytes

Chondrocytes were isolated and cultured as described before [34]. All animal experimental procedures were performed in accordance with U.K. Animals (Scientific Procedures) Act, 1986 and European guidelines (2010/63/EU) and approved by the Experimental Animal Ethics Committee of Tongji Medical College, Huazhong University of Science and Technology, Wuhan, China. In brief, cartilage was removed from the knee joints of 5 days old C57BL/6J mice (the sex cannot be identified at this age). After dissected into pieces, cartilage was respectively digested with 0.25% trypsin for 30 min and 0.25% type 2 collagenase for 6 h. The primary chondrocytes were resuspended and cultured in DMEM/F12 medium containing 10% foetal bovine serum (FBS), 1% penicillin and 1% streptomycin sulfate at 37 °C under 5% CO₂. Chondrocytes at second passage were used in experiments.

Western blot analysis

Chondrocytes were seeded in 6-well plates at a density of 5×10^5 cells/well and adhered for 24 h. Then, cells were subjected to different treatments. In the first group, chondrocytes were treated with 100 μ M FAC for 48 h. In the second group, chondrocytes were treated with 10 ng/mL IL-1 β for 48 h. In the third group, chondrocytes were treated with 5 μ M erastin for 48 h. In the last group, chondrocytes were treated by 100 μ M FAC or 10 ng/mL IL-1 β with 1 μ M ferrostatin-1 or equal volume of DMSO for 48 h. Western Blot analysis was performed as described before [35]. In brief, chondrocytes were washed three times with PBS and then lysed with 100 μ l RIPA lysis buffer (Boster, China, AR0102) that containing 1% proteinase inhibitor cocktail for 30 min on ice. After centrifugation at 13,000 rpm for 20 min, the supernatant was collected and the protein concentration of each sample was detected by BCA assay kit (Boster, China, AR0146). Equal quality of proteins (25 μ g) was electrophoresis in 12% SDS-PAGE gel, and transferred to the PVDF membranes (Millipore, United States). After blocking with 5% skim milk at room temperature for 1 h, the membranes were incubated with primary antibodies overnight at 4 °C and incubated with secondary antibodies for 1 h at room temperature. Protein bands were visualized using chemiluminescence substrate kit (Boster, China) and ChemiDocTM XRS + System (Bio-Rad Laboratories, CA, United States). The density of each band was quantified by image J version 1.48.

Immunofluorescence staining

Chondrocytes were seeded into 24-well plates. After treatment, cells were fixed by 4% paraformaldehyde for 15 min at room temperature. Then, cells were permeabilized 0.5% Triton X-100 for 20 min and blocked with 5% BSA for 1 h at room temperature. Chondrocytes were then incubated with GPX4 antibodies overnight at 4 °C. On the second day, cells were incubated with Cy3-conjugated goat anti-rabbit secondary antibody for 1 h in the dark. After washed three times with PBS, cells were incubated with DAPI for 5 min. Images were obtained under the fluorescence microscope (EvoS fl auto, Life technologies, USA).

Cell viability assay

The chondrocytes viability was detected using cell counting kit-8 (CCK-8) (Boster, China, AR1160). Chondrocytes were seeded into 96-well plates at a density of 3000 cells/well. After adherence for 24 h, cells were treated by 100 μ M FAC or 10 ng/mL IL-1 β with 1 μ M ferrostatin-1 or equal volume of DMSO for 48 h. After removal of medium, 100 μ l of 10% CCK-8 solution was added to each well and incubated at 37 °C away from light for 2 h. The absorbance was measured at 450 nm using a microplate reader (Thermo Fisher Scientific, Vantaa, Finland).

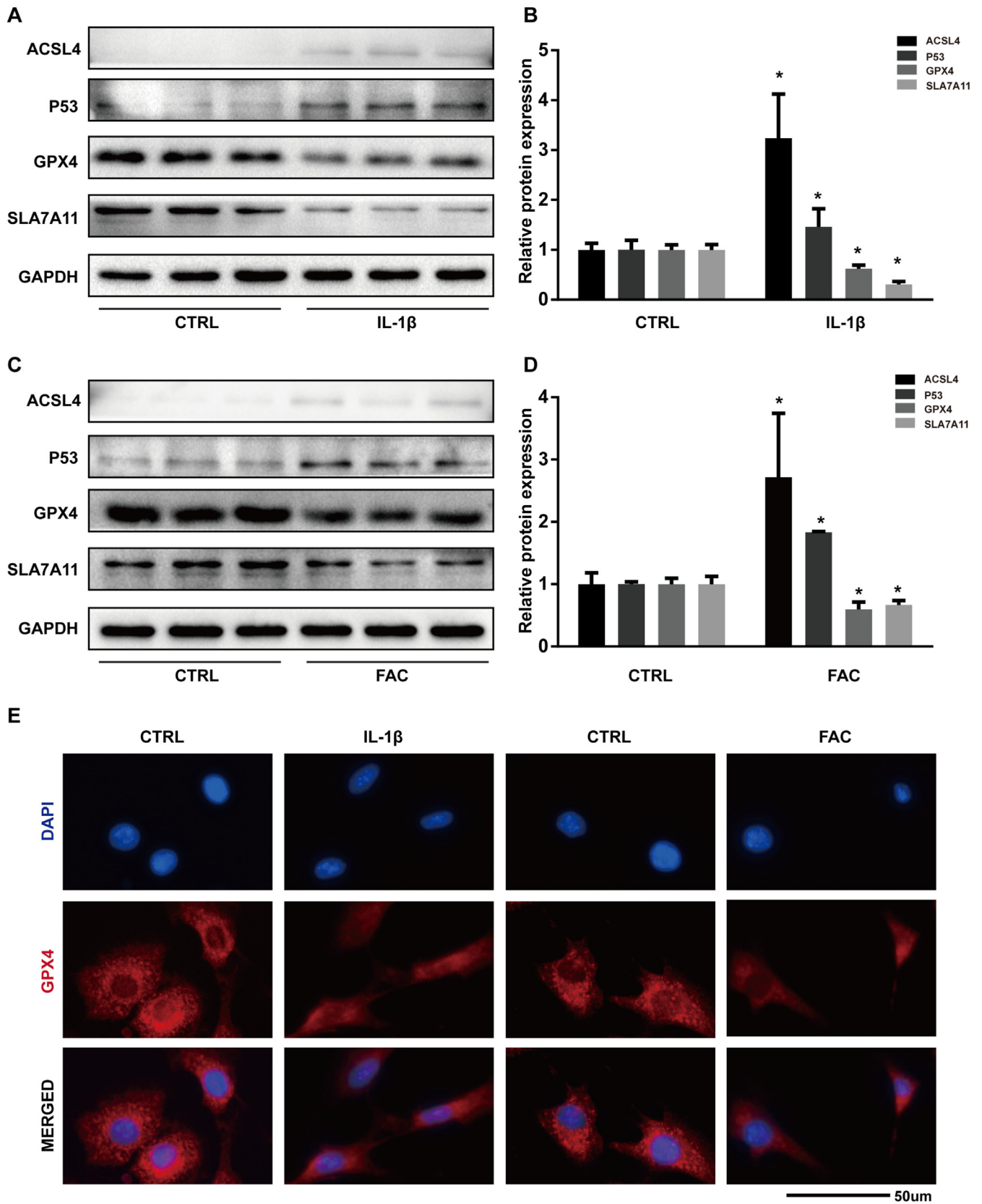
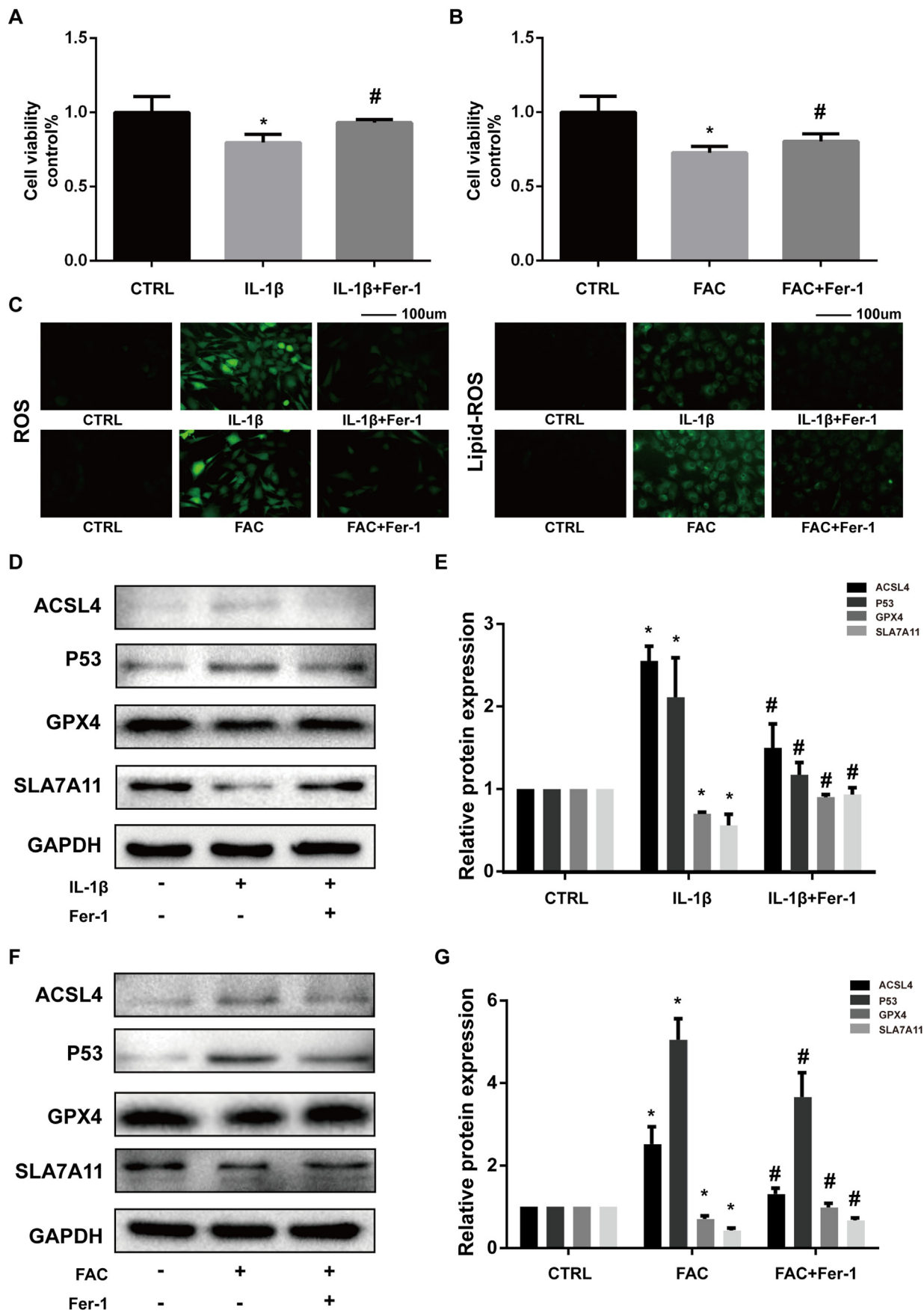


Figure 1. Both IL-1β and FAC induced ferroptosis related protein expression changes in chondrocytes (A) The protein expression level of ACSL4, GPX4, P53, and SLC7A11, when treated with IL-1β, were detected by western blot (B) Band density ratios of ACSL4, GPX4, P53, and SLC7A11 to GAPDH in the western blots were quantified by densitometry (C) The protein expression level of ACSL4, GPX4, P53, and SLC7A11 when treated with FAC were detected by western blot (D) Band density ratios of ACSL4, GPX4, P53 and SLC7A11 to GAPDH in the western blots were quantified by densitometry (E) Total GPX4 protein level were evaluated by immunofluorescence staining in chondrocytes treated with IL-1β or FAC. *P < 0.05 versus control. Error bars represent SD.



(caption on next page)

Figure 2. Ferrostatin-1 attenuated the cytotoxicity, ROS and lipid-ROS accumulation and ferroptosis related protein expression changes induced by IL-1 β and FAC (A–B) Cell viability determined by CCK-8 assay (C) Intracellular ROS and lipid-ROS level detected by DCFH-DA and C11 BODIPY fluorescent probe (D) The protein expression level of ACSL4, GPX4, P53, and SLC7A11 when treated by IL-1 β with 1 μ M ferrostatin-1 or equal volume of DMSO were detected by western blot (E) Band density ratios of ACSL4, GPX4, P53 and SLC7A11 to GAPDH in the western blots were quantified by densitometry (F) The protein expression level of ACSL4, GPX4, P53 and SLC7A11 when treated by FAC with 1 μ M ferrostatin-1 or equal volume of DMSO were detected by western blot (G) Band density ratios of ACSL4, GPX4, P53 and SLC7A11 to GAPDH in the western blots were quantified by densitometry. *P < 0.05 versus control, #P < 0.05 versus IL-1 β or FAC treated group. Error bars represent SD.

Detection of intracellular ROS and lipid-ROS

Chondrocytes were firstly seeded in 6-well plates at a density of 3×10^5 cells/well. After 24 h, chondrocytes were treated by 100 μ M FAC or 10 ng/mL IL-1 β with 1 μ M ferrostatin-1 or equal volume of DMSO for 48 h. The intracellular ROS and lipid-ROS levels were measured with the DCFH-DA and C11 BODIPY fluorescent probe according to the manufacturer's instructions. In brief, chondrocytes were washed with PBS three times and treated with 10 μ M DCFH-DA or 5 μ M of C11 BODIPY for 20 min at 37 °C in the dark. After incubation, cells were washed with PBS and observed under the fluorescence microscope (Evos fl auto, life technologies, USA).

Nuclear protein extraction

The nuclear protein was extracted using a nuclear protein extraction kit (Beyotime, China, P0028) according to the manufacturer's protocol. The nuclear protein was subjected to western blot analysis and lamin B were used as internal control.

Knockdown of Nrf2 by small interfering RNA

Specific small interfering RNA (siRNA) targeting the mouse Nrf2 gene was chemically synthesized by RiboBio (Guangzhou, China) and was transfected into cells using Lipofectamine 3000 transfection reagent following the manufacturer's instructions (Thermo Fisher, UT, USA). The siRNA sequences and knockdown efficiency was reported in our previous article [34]. The sense strand sequences of Nrf2 siRNA are as follows: 5'-CGACAGAC CCTCCATCTA-3'.

Animal experiment

Thirty-two 8 weeks old male C57BL/6 mice were used in this study. Eight mice were randomly allocated to the sham surgery group. After anesthetized by intraperitoneal injection of pentobarbital (35 mg/kg), sham surgery group were subjected to sham surgery. Then, destabilized medial meniscus (DMM) were performed to establish the OA model in twenty-four mice. DMM mice were randomly divided into three groups (N = 8 for each group): the DMM group, the DMM+0.1 mg/kg ferrostatin-1 group and the DMM+1 mg/kg ferrostatin-1 group. The DMM+0.1 mg/kg ferrostatin-1 group and the DMM+1 mg/kg ferrostatin-1 group were intraarticularly injected with 0.1 mg/kg or 1 mg/kg ferrostatin-1 respectively. The sham surgery group and DMM group were intraarticularly injected with same volume of vehicle. The injection was repeated twice a week for 8 consecutive weeks. Eight weeks later, mice were sacrificed and the knee joints were collected and fixed in 4% paraformaldehyde for further experiments.

Histological and immunohistochemical staining

Knee joints were decalcified with 10% EDTA solution for two weeks and embedded in paraffin wax. The specimens were sectioned to 5 μ m thickness in a sagittal plane and then stained with Safranin O/fast green. The progression of OA was evaluated using the Osteoarthritis Research Society International (OARSI) scores in a blind manner. Other sections were deparaffinized, antigen retrieved, incubated with anti-GPX4 or anti-Collagen II antibody, and then incubated with goat anti-rabbit secondary antibody. Sections were colored with DAB and counterstained with

hematoxylin. The image was captured by fluorescence microscope (Evos fl auto, Life technologies, USA) and the number of GPX4 or collagen II positive cell per field in each group were counted under 200-time magnification.

Statistical analysis

All the data were presented as the means \pm standard deviation (SD). Statistical analyses were performed using GraphPad Prism version 6.05. Differences in numerical data between two groups were determined by Student's two-tailed t-test. One-way ANOVA was used to determine differences among groups more than two followed by a Bonferroni post hoc test. P < 0.05 was defined as statistically significant.

Results

Both IL-1 β and FAC induced ferroptosis related protein expression changes in chondrocytes

In this study, we used the protein expression level of GPX4, ACSL4, P53, and SLC7A11 as markers of ferroptosis. The results of western blot showed that both IL-1 β and FAC could suppress the expression of GPX4 and SLC7A11 while increased the protein level of P53 and ACSL4 in chondrocytes (Fig. 1A and C). Band density ratios of ACSL4, GPX4, P53, and SLC7A11 to GAPDH in the western blots were quantified by densitometry. The difference in protein band density ratio is statistically significant (Fig. 1B and D). In addition, we visualized the total protein level of GPX4 by immunofluorescence staining. In the control group, the red fluorescence (which indicated the GPX4 protein) is aggregated in mitochondria to form granular dots and diffusely distributed in the cytoplasm. When treated by IL-1 β or FAC, the intensity of red fluorescence is reduced and the number of red granular dots was decreased (Fig. 1E). Together, those results proved that both IL-1 β and FAC induced ferroptosis related protein expression changes in chondrocytes.

Ferrostatin-1 attenuated the cytotoxicity, ROS, and lipid-ROS accumulation and ferroptosis related protein expression changes induced by IL-1 β and FAC

Ferrostatin-1 is an efficient ferroptosis specific inhibitor functioned by eliminating the initiating alkoxy radicals and other rearrangement products that produced by ferrous iron from lipid hydroperoxides [36]. We used Ferrostatin-1 to verify the existence of ferroptosis in IL-1 β and FAC treated chondrocytes. Both IL-1 β and FAC exerted significant cytotoxicity to chondrocytes according to CCK-8 assay. Ferrostatin-1 could partly attenuate the cytotoxicity (Fig. 2A and B). Also, we used DCFH-DA and C11 BODIPY fluorescent probe to detect the intracellular ROS and lipid-ROS. The results showed that both the ROS and lipid-ROS is accumulated in chondrocytes when treated with IL-1 β or FAC (reflected by the intensity of green fluorescence). Ferrostatin-1 can reduce the intracellular ROS and lipid-ROS levels (Fig. 2C). In addition, Ferrostatin-1 could rescue the expression of GPX4 and SLC7A11 and attenuate the expression for P53 and ACSL4 (Fig. 2D and F). The difference in protein band density ratio is statistically significant (Fig. 2E and G). We also visualized the total protein level of GPX4 by immunofluorescence staining. The results show that ferrostatin-1 can increase the number of red granular dots and enhanced the intensity of red fluorescence (Fig. 3). This phenomenon indicated that ferrostatin-1 can rescue the GPX4

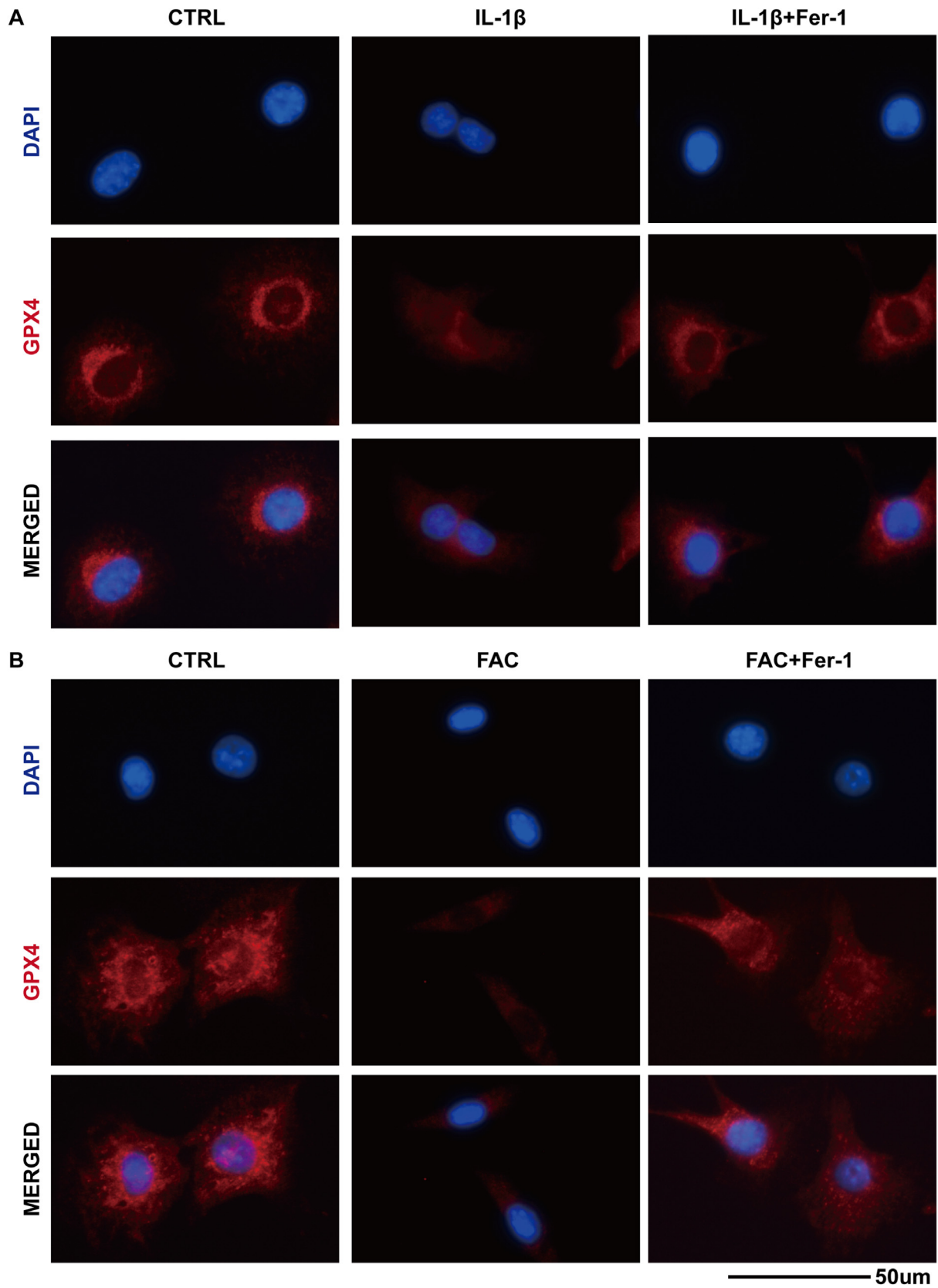


Figure 3. (A) The total GPX4 protein level in the chondrocytes treated with IL-1 β or in combination with ferrostain-1 was evaluated by immunofluorescence staining. The nuclei were stained with DAPI (B) The total GPX4 protein level in the chondrocytes treated with FAC or in combination with ferrostain-1 were evaluated by immunofluorescence staining. The nuclei were stained with DAPI.

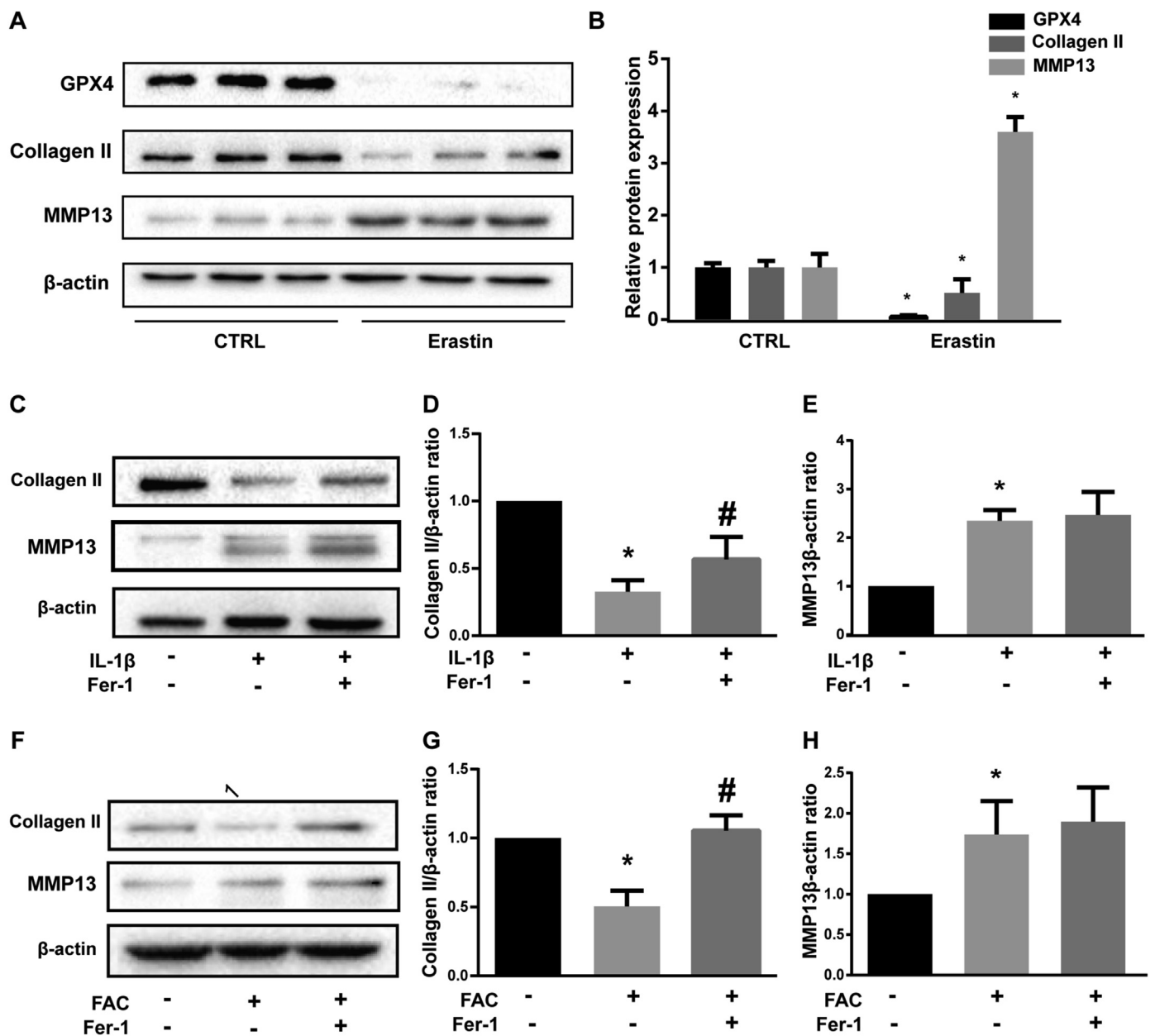


Figure 4. Erastin promoted matrix metalloproteinase 13 (MMP13) expression while inhibited Type II collagen (collagen II) expression in chondrocytes (A) The protein expression level of GPX4, collagen II and MMP13 when treated with erastin were detected by western blot (B) The band density ratio of GPX4, collagen II and MMP13 to β-actin in the western blots were quantified by densitometry (C) The protein expression level of collagen II and MMP13 when treated by IL-1β with 1 μM ferrostatin-1 or equal volume of DMSO were detected by western blot (D-E) The band density ratio of collagen II and MMP13 to β-actin in the western blots were quantified by densitometry (F) The protein expression level of collagen II and MMP13 when treated by FAC with 1 μM ferrostatin-1 or equal volume of DMSO were detected by western blot (G-H) The band density ratio of collagen II and MMP13 to β-actin in the western blots were quantified by densitometry. *P < 0.05 versus control, #P < 0.05 versus IL-1β or FAC treated group. Ns P > 0.05 versus IL-1β or FAC treated group. Error bars represent SD.

expression that suppressed by IL-1β and FAC. Above results combined, we proved that both IL-1β and FAC could induce chondrocytes ferroptosis.

Erastin promoted matrix metalloproteinase 13 (MMP13) expression while inhibited type II collagen (collagen II) expression in chondrocytes

Collagen II, which is secreted by chondrocytes, is the major component of ECM. MMP13, the major ECM-degrading enzyme, is significantly over-expressed in osteoarthritic articular cartilage and basically undetectable in normal adult tissues [37,38]. Hence, decreased collagen II and increased MMP13 secretion by chondrocytes are major biomarkers and contributors of OA. Erastin is the most classic inducer of ferroptosis [39].

High efficiency of erastin was confirmed by significantly suppressed GPX4 protein level (Fig. 4A and B). When chondrocytes were treated with erastin, collagen II expression was significantly suppressed while MMP13 expression was evaluated (Fig. 4A and B). Further, we proved that ferrostatin-1 rescued the collagen II expression that suppressed by IL-1β and FAC (Fig. 4C and F). The difference of protein band density ratio of collagen II to β-actin is statistically significant (Fig. 4D and G). However, ferrostatin-1 did not attenuate the expression of MMP13 induced by IL-1β and FAC (Fig. 4E and H). Considering Ferrostatin-1 inhibits ferroptosis by eliminating lipid ROS, We speculated that ferroptosis might induce the MMP13 expression in a lipid ROS independent way.

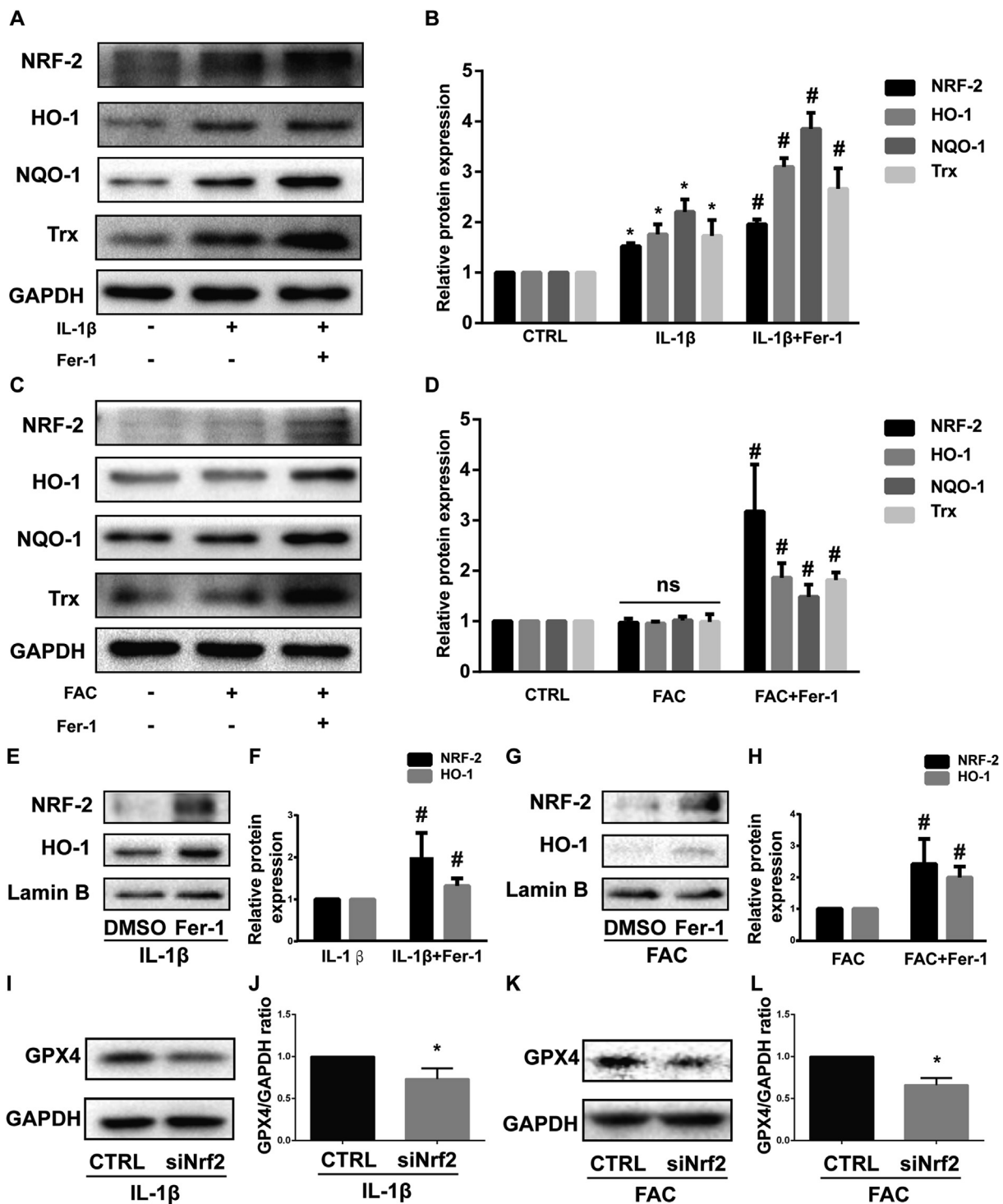


Figure 5. Nrf2 antioxidant system and ferroptosis are mutually regulated under inflammation and iron overload condition (A) The protein expression level of Nrf2, HO-1, NQO-1 and Trx when treated by IL-1β with 1 μM ferrostatin-1 or equal volume of DMSO were detected by western blot (B) The band density ratio of Nrf2, HO-1, NQO-1 and Trx to GAPDH in the western blots were quantified by densitometry (C) The protein expression level of Nrf2, HO-1, NQO-1 and Trx when treated by FAC with 1 μM ferrostatin-1 or equal volume of DMSO were detected by western blot (D) The band density ratio of Nrf2, HO-1, NQO-1 and Trx to GAPDH in the western blots were quantified by densitometry. (E) The nuclear protein level of Nrf2 and HO-1 when treated by IL-1β with 1 μM ferrostatin-1 or equal volume of DMSO were detected by western blot (F) The band density ratio of Nrf2 and HO-1 to Lamin B were quantified by densitometry. (G) The nuclear protein level of Nrf2 and HO-1 when treated by FAC with 1 μM ferrostatin-1 or equal volume of DMSO were detected by western blot (H) The band density ratio of Nrf2 and HO-1 to Lamin B were quantified by densitometry. (I) The protein level of GPX4 when treated by IL-1β with siNrf2 or negative control were detected by western blot (J) The band density ratio of GPX4 to GAPDH were quantified by densitometry. (K) The protein level of GPX4 when treated by IL-1β with siNrf2 or negative control were detected by western blot (L) The band density ratio of GPX4 to GAPDH were quantified by densitometry. *P < 0.05 versus control, #P < 0.05 versus IL-1β or FAC treated group. ns P > 0.05. Error bars represent SD.

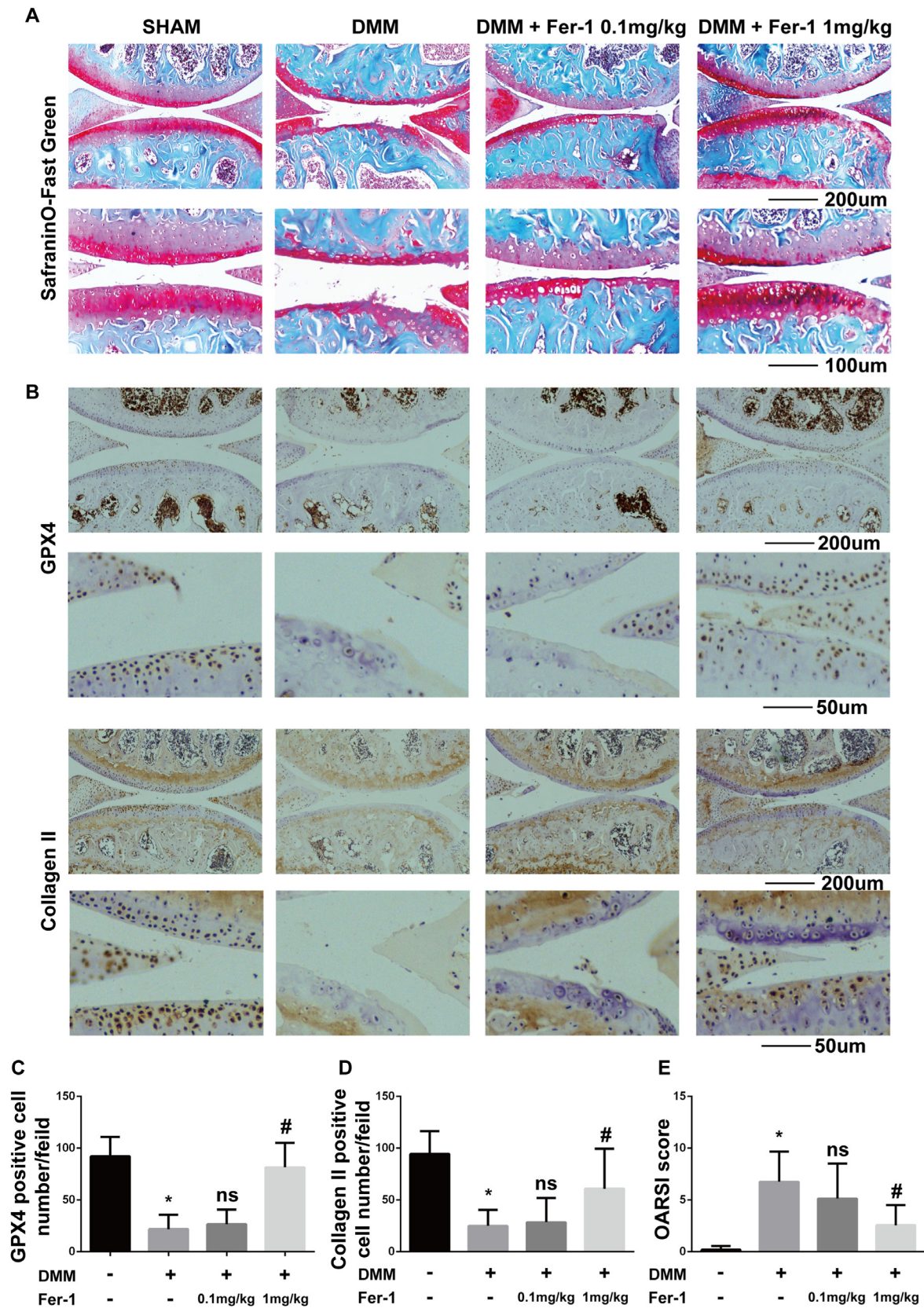


Figure 6. Ferrostatin-1 attenuated cartilage degradation and increased the Collagen II and GPX4 expression in the mouse OA model (A) Cartilage degradation was assessed by Safranin O/fast green staining (B) Immunohistochemistry staining of GPX4 and collagen II (C) Number of GPX4 positive cells per field under 200-time magnification (D) The number of collagen positive cells per field under 200-time magnification (E) The progression of OA was evaluated using the OARSI scores. *P < 0.05 versus sham surgery group, #P < 0.05 versus DMM group. ns P > 0.05. Error bars represent SD.

Nrf2 antioxidant system and ferroptosis are mutually regulated under inflammation and iron overload condition

Nrf2 (NF-E2-related factor 2) and its downstream effectors such as HO-1, NQO-1, and Trx are the main cellular antioxidant system [40]. Also, Nrf2 is identified as a key factor that mitigates lipid peroxidation and ferroptosis [41]. When activated, Nrf2 translocates from the cytoplasm to the nucleus and then activates target antioxidant enzyme genes by binding to the antioxidant response element (ARE) [42]. In our study, IL-1 β treatment increased the total protein level of Nrf2, HO-1, NQO-1, and Trx while the expression of those proteins didn't alter obviously when treated with FAC. Ferrostatin-1 was able to further enhance the expression of Nrf2, HO-1, NQO-1 and Trx (Fig. 5A and C). The difference in protein band density ratio is statistically significant (Fig. 5B and D). In addition, ferrostatin-1 also increased the intranuclear Nrf2 and HO-1 protein (which also translate into to nucleus when activated) level determined by western blot (Fig. 5E and G). The difference of protein band density ratio is statistically significant (Fig. 5F and H). This phenomenon indicated that ferrostatin-1 facilitated the activation of the Nrf2 antioxidant system in chondrocytes. Moreover, we knockdown Nrf2 with siRNA when chondrocytes were treated with IL-1 β or FAC. High knockdown efficiency was verified by western blot as described in our previous article [34]. The results showed that knockdown of Nrf2 decreased the GPX4 expression level which indicated higher ferroptosis rates (Fig. 5I and K). The difference in protein band density ratio of GPX4 to GAPDH is statistically significant (Fig. 5J and L). Those results combined indicated that the Nrf2 antioxidant system and ferroptosis are mutually regulated under inflammation and iron overload condition, although the detailed mechanism is still unclear.

Ferrostatin-1 attenuated cartilage degradation and increased the collagen II and GPX4 expression in mouse OA model

Considering that both IL-1 β (inflammation) and FAC (iron overload) induced chondrocytes ferroptosis *in vitro*, we further investigated whether ferroptosis specific inhibitor ferrostatin-1 could attenuate OA progression *in vivo*. We used the surgery-induced DMM mouse model to induce OA *in vivo*. Intraarticular injection of 1 mg/kg ferrostatin-1 significantly attenuated cartilage degradation assessed by Safranin O/fast green staining (Fig. 6A). Immunohistochemistry staining of GPX4 was used to evaluate the ferroptosis level of chondrocyte. The number of GPX4 positive cells was reduced in the DMM group and intraarticular injection of 1 mg/kg ferrostatin-1 increased the GPX4 positive cell number with statistical significance (Fig. 6B and C, Fig. S1). This result suggested that ferroptosis was induced by DMM and the efficiency of ferroptosis inhibition by ferrostatin-1 is promising *in vivo*. In addition, we found that intraarticular injection of 1 mg/kg ferrostatin-1 rescued the expression of collagen II which is consistent with our *in vitro* experiment (Fig. 6B and D, Fig. S1). We also evaluated the severity of OA using the OARSI score. The results showed that intraarticular injection of 1 mg/kg ferrostatin-1 attenuated OA progression with statistical significance (Fig. 6E). In summary, inhibition of ferroptosis by ferrostatin-1 attenuated OA progression in the DMM mice model.

Discussion

OA is the most prevalent joint disease with an increasing trend. Previous studies suggested that necrosis, apoptosis and autophagic cell death of chondrocytes contribute to the development of OA. Ferroptosis is proved to be correlated with many pathological conditions such as Alzheimer's disease, Parkinson's diseases, carcinogenesis, intracerebral hemorrhage, traumatic brain injury, ischemia-reperfusion injury, and stroke. Hence, inhibition of ferroptosis represents a novel and attractive therapeutic method for those diseases. However, if ferroptosis is involved in the progression of OA is still unknown.

According to the guideline of the Nomenclature Committee on Cell

Death, ferroptosis is defined as a form of regulated cell death initiated by oxidative perturbations of the intracellular microenvironment that is under constitutive control by GPX4 and can be inhibited by iron chelators and lipophilic antioxidants [20]. In our current study, we tried to verify the chondrocytes ferroptosis by its definition. Firstly, we accessed the oxidative perturbations by detecting the intracellular ROS and lipid-ROS level. Secondly, we detected the protein expression level of GPX4 along with three other well recognized ferroptotic biomarkers and contributors (ACSL4, P53, and SLC7A11) by western blot. Lastly, we used ferroptosis specific inhibitor ferrostatin-1 to verify the ferroptosis in both *vivo* and *vitro*. Moreover, erastin, the most classic ferroptosis inducer, decreased the collagen II expression and increased the MMP13 expression. Ferrostatin-1 could rescue the collagen II expression in both *vivo* and *vitro* and attenuate cartilage degradation *in vivo*. However, ferrostatin-1 didn't attenuate erastin induced MMP13 expression. Ferrostatin-1 inhibits ferroptosis by eliminating the initiating alkoxy radicals and other rearrangement products that produced by ferrous iron from lipid hydroperoxides [39]. Thus, we speculated that ferroptosis might induce the MMP13 expression in a lipid ROS independent way. Although ferroptosis is characterized by highly iron-dependent lipid peroxidation, it also involves various biological processes such as oxidative stress, lipid metabolism, iron metabolism and biosynthesis of NADPH, glutathione and coenzyme Q10 [43]. The mechanism of erastin induced MMP13 expression still remains unclear and required further study. Together, our study proved that ferroptosis is involved in the progression of OA. As far as we knew, our study is the first one that demonstrated ferroptosis of chondrocytes is participate in the progression of OA and the first one that proved ferrostatin-1 exerted anti-osteoarthritic effect *in vivo* and attenuated IL-1 β and FAC induced chondrocyte dysfunction *in vitro*.

Nrf2, the main cellular antioxidant system, is a key factor that mitigates ferroptosis. In our study, we found that Ferrostatin-1 facilitated the expression of Nrf2 and its downstream effectors and the nuclear translocation of Nrf2 and HO1 when chondrocytes were treated with IL-1 β or FAC. Such a phenomenon suggested that ferroptosis limited the activation of Nrf2 in response to oxidative stress. In addition, knockdown of Nrf2 decreased the GPX4 protein level in chondrocytes when treated with IL-1 β or FAC. These results indicated that Nrf2 is required for chondrocytes to limited ferroptosis which were consistent with previous studies [44]. In summary, the results of our study suggested that the Nrf2 antioxidant system and ferroptosis were mutually regulated under inflammation and iron overload condition. However, the detailed mechanism remains unclear. We think the interaction between ferroptosis and Nrf2 is of interest and worth to be further studied in the future.

Our study has some limitations. Firstly, unlike apoptosis, there is still no golden standard for the detection of ferroptosis. However, we do verify ferroptosis by its definition that defined by the Nomenclature Committee on Cell Death and preliminarily demonstrated that ferroptosis is involved in the progression of OA *in vivo* and correlated with increased MMP13 expression and decreased collagen II expression *in vitro*. Secondly, Adult human chondrocytes basically do not proliferate and the development of OA and often takes years or even decades. Thus, chondrocyte injures and cell death will accumulate during the progression of OA. In our experiment, we only treated chondrocytes for 48 h. Moreover, the mice chondrocytes we used in our *in vitro* experiments are proliferative. The chondrocytes ferroptosis can be partly rescued by cell proliferation. Thus, the chondrocyte ferroptosis were underestimated in our study. This limitation also leads to the reduction of cell viability induced by IL-1 β and FAC and its rescue by Ferrostatin-1 is not very dramatic in our CCK-8 assay. This limitation also exists during the study of chondrocyte apoptosis. However, the result is statistically significant and the limitation doesn't impair the conclusion.

In summary, we firstly proved that chondrocytes underwent ferroptosis under inflammation and iron overload condition and ferroptosis contributed to the progression of osteoarthritis *in vivo* and promoted MMP13 expression while inhibited collagen II expression in chondrocytes cultured *in vitro*. The inhibition of ferroptosis seems to be a

novel and promising therapeutic option for OA.

Funding

The study was funded by the National Natural Science Foundation of China (No. 81874020 and NO. 81702155).

Declaration of competing interest

The authors declare that they have no conflicts of interest.

Acknowledgements

Thanks to the support from the National Natural Science Foundation of China.

Appendix A. Supplementary data

Supplementary data to this article can be found online at <https://doi.org/10.1016/j.jot.2020.09.006>.

References

- [1] James SL, Abate D, Abate KH, Abay SM, Abbafati C, Abbasi N, et al. Global, regional, and national incidence, prevalence, and years lived with disability for 354 diseases and injuries for 195 countries and territories, 1990–2017: a systematic analysis for the Global Burden of Disease Study 2017. *LANCET (N AM ED)* 2018; 392(10159):1789–858. 2018-11-10.
- [2] Musumeci G, Aiello FC, Szychlinska MA, Di Rosa M, Castrogiovanni P, Mobasher A. Osteoarthritis in the XXIst century: risk factors and behaviours that influence disease onset and progression. *Int J Mol Sci* 2015;16(3):6093–112. 2015-03-16.
- [3] Mobasher A, Batt M. An update on the pathophysiology of osteoarthritis. *Ann Phys Rehabil Med* 2016;59(5–6):333–9. 2016-12-01.
- [4] Abramoff B, Caldera FE. Osteoarthritis: pathology, diagnosis, and treatment options. *Med Clin* 2020;104(2):293–311. 2020-03-01.
- [5] Gozzelino R, Arosio P. Iron homeostasis in health and disease. *Int J Mol Sci* 2016; 17(1). 2016-01-20.
- [6] Li C, Ouyang N, Wang X, Liang A, Mo Y, Li S, et al. Association between the ABO blood group and primary knee osteoarthritis: a case-control study. *J Orthop Translat* 2020;21:129–35. 2020.
- [7] Tong W, Zeng Y, Chow D, Yeung W, Xu J, Deng Y, et al. Wnt16 attenuates osteoarthritis progression through a PCP/JNK-mTORC1-PTHrP cascade. *Ann Rheum Dis* 2019;78(4):551–61. 2019.
- [8] Lefebvre V, Dvir-Ginzberg M. SOX9 and the many facets of its regulation in the chondrocyte lineage. *Connect Tissue Res* 2017;58(1):2–14. 2017-01-01.
- [9] Sellam J, Berenbaum F. The role of synovitis in pathophysiology and clinical symptoms of osteoarthritis. *Nat Rev Rheumatol* 2010;6(11):625–35. 2010-11-01.
- [10] Jenei-Lanzl Z, Meurer A, Zaucke F. Interleukin-1beta signaling in osteoarthritis - chondrocytes in focus. *Cell Signal* 2019;53:212–23. 2019-01-01.
- [11] Goldring MB, Otero M. Inflammation in osteoarthritis. *Curr Opin Rheumatol* 2011; 23(5):471–8. 2011-09-01.
- [12] Garcia-Gil M, Reyes C, Ramos R, Sanchez-Santos MT, Prieto-Alhambra D, Spector TD, et al. Serum lipid levels and risk of hand osteoarthritis: the chingford prospective cohort study. *Sci Rep* 2017;7(1):3147. 2017-06-09.
- [13] Frey N, Hugle T, Jick SS, Meier CR, Spoendlin J. Hyperlipidaemia and incident osteoarthritis of the hand: a population-based case-control study. *Osteoarthritis Cartilage* 2017;25(7):1040–5. 2017-07-01.
- [14] Camacho A, Simao M, Ea HK, Cohen-Solal M, Richette P, Branco J, et al. Iron overload in a murine model of hereditary hemochromatosis is associated with accelerated progression of osteoarthritis under mechanical stress. *Osteoarthritis Cartilage* 2016;24(3):494–502. 2016-03-01.
- [15] Sinigaglia L, Fargion S, Fracanzani AL, Binelli L, Battafarano N, Varenna M, et al. Bone and joint involvement in genetic hemochromatosis: role of cirrhosis and iron overload. *J Rheumatol* 1997;24(9):1809–13. 1997-09-01.
- [16] Carroll GJ, Breidahl WH, Bulsara MK, Olynnyk JK. Hereditary hemochromatosis is characterized by a clinically definable arthropathy that correlates with iron load. *Arthritis Rheum* 2011;63(1):286–94. 2011-01-01.
- [17] Sandell LJ, Aigner T. Articular cartilage and changes in arthritis. An introduction: cell biology of osteoarthritis. *Arthritis Res* 2001;3(2):107–13. 2001-01-20.
- [18] Jiang S, Liu Y, Xu B, Zhang Y, Yang M. Noncoding RNAs: new regulatory code in chondrocyte apoptosis and autophagy. *Wiley Interdiscip Rev RNA*; 2020. 2020-01-10:e1584.
- [19] Dixon SJ, Lemberg KM, Lamprecht MR, Skouta R, Zaitsev EM, Gleason CE, et al. Ferroptosis: an iron-dependent form of nonapoptotic cell death. *Cell* 2012;149(5): 1060–72. 2012-05-25.
- [20] Seibt TM, Proneth B, Conrad M. Role of GPX4 in ferroptosis and its pharmacological implication. *Free Radic Biol Med* 2019;133:144–52. 2019-03-01.
- [21] Doll S, Proneth B, Tyurina YY, Panzilius E, Kobayashi S, Ingold I, et al. ACSL4 dictates ferroptosis sensitivity by shaping cellular lipid composition. *Nat Chem Biol* 2017;13(1):91–8. 2017-01-01.
- [22] Yuan H, Li X, Zhang X, Kang R, Tang D. Identification of ACSL4 as a biomarker and contributor of ferroptosis. *Biochem Biophys Res Commun* 2016;478(3):1338–43. 2016-09-23.
- [23] Lewerenz J, Hewett SJ, Huang Y, Lambros M, Gout PW, Kalivas PW, et al. The cystine/glutamate antiporter system x(c)(-) in health and disease: from molecular mechanisms to novel therapeutic opportunities. *Antioxidants Redox Signal* 2013; 18(5):522–55. 2013-02-10.
- [24] Jiang L, Kon N, Li T, Wang SJ, Su T, Hibshoosh H, et al. Ferroptosis as a p53-mediated activity during tumour suppression. *NATURE* 2015;520(7545):57–62. 2015-04-02.
- [25] Galluzzi L, Vitale I, Aaronson SA, Abrams JM, Adam D, Agostinis P, et al. Molecular mechanisms of cell death: recommendations of the nomenclature committee on cell death 2018. *Cell Death Differ* 2018;25(3):486–541. 2018-03-01.
- [26] Stockwell BR, Friedmann AJ, Bayir H, Bush AI, Conrad M, Dixon SJ, et al. Ferroptosis: a regulated cell death nexus linking metabolism, redox biology, and disease. *Cell* 2017;171(2):273–85. 2017-10-05.
- [27] van Vulpen LF, Roosendaal G, van Asbeck BS, Mastbergen SC, Lafeber FP, Schutgens RE. The detrimental effects of iron on the joint: a comparison between haemochromatosis and haemophilia. *J Clin Pathol* 2015;68(8):592–600. 2015-08-01.
- [28] Nieuwenhuizen L, Schutgens RE, van Asbeck BS, Wenting MJ, van Veghel K, Roosendaal G, et al. Identification and expression of iron regulators in human synovium: evidence for upregulation in haemophilic arthropathy compared to rheumatoid arthritis, osteoarthritis, and healthy controls. *Haemophilia* 2013;19(4): e218–27. 2013-07-01.
- [29] Koorts AM, Levay PF, Hall AN, van der Merwe CF, Becker PJ, Frantzen DJ, et al. Expression of the H- and L-subunits of ferritin in bone marrow macrophages of patients with osteoarthritis. *Exp Biol Med* 2012 2012-06-01;237(6):688–93.
- [30] Abusarah J, Bentz M, Benabdoune H, Rondon PE, Shi Q, Fernandes JC, et al. An overview of the role of lipid peroxidation-derived 4-hydroxynonenal in osteoarthritis. *Inflamm Res* 2017;66(8):637–51. 2017-08-01.
- [31] Yu T, Qu J, Wang Y, Jin H. Ligustrazine protects chondrocyte against IL-1beta induced injury by regulation of SOX9/NF-kappaB signaling pathway. *J Cell Biochem* 2018;119(9):7419–30. 2018-09-01.
- [32] Yao X, Zhang J, Jing X, Ye Y, Guo J, Sun K, et al. Fibroblast growth factor 18 exerts anti-osteoarthritic effects through PI3K-AKT signaling and mitochondrial fusion and fission. *Pharmacol Res* 2019;139:314–24. 2019-01-01.
- [33] Qiu L, Luo Y, Chen X. Quercetin attenuates mitochondrial dysfunction and biogenesis via upregulated AMPK/SIRT1 signaling pathway in OA rats. *Biomed Pharmacother* 2018;103:1585–91. 2018-07-01.
- [34] Sun K, Luo J, Jing X, Guo J, Yao X, Hao X, et al. Astaxanthin protects against osteoarthritis via Nrf2: a guardian of cartilage homeostasis. *Aging (Albany NY)* 2019;11(22):10513–31. 2019-11-26.
- [35] Yao X, Jing X, Guo J, Sun K, Deng Y, Zhang Y, et al. Icarin protects bone marrow mesenchymal stem cells against iron overload induced dysfunction through mitochondrial fusion and fission, PI3K/AKT/mTOR and MAPK pathways. *Front Pharmacol* 2019;10:163. 2019-01-20.
- [36] Miotto G, Rossetto M, Di Paolo ML, Orian L, Venerando R, Roveri A, et al. Insight into the mechanism of ferroptosis inhibition by ferrostatin-1. *REDOX BIOL* 2020;28: 101328. 2020-01-01.
- [37] Knauper V, Cowell S, Smith B, Lopez-Otin C, O'Shea M, Morris H, et al. The role of the C-terminal domain of human collagenase-3 (MMP-13) in the activation of procollagenase-3, substrate specificity, and tissue inhibitor of metalloproteinase interaction. *J Biol Chem* 1997;272(12):7608–16. 1997-03-21.
- [38] Vincenti MP, Brinckerhoff CE. Transcriptional regulation of collagenase (MMP-1, MMP-13) genes in arthritis: integration of complex signaling pathways for the recruitment of gene-specific transcription factors. *Arthritis Res* 2002;4(3):157–64. 2002-01-20.
- [39] Dixon SJ, Lemberg KM, Lamprecht MR, Skouta R, Zaitsev EM, Gleason CE, et al. Ferroptosis: an iron-dependent form of nonapoptotic cell death. *Cell* 2012;149(5): 1060–72. 2012-05-25.
- [40] Rojo DLVM, Chapman E, Zhang DD. NRF2 and the hallmarks of cancer. *Canc Cell* 2018;34(1):21–43. 2018-07-09.
- [41] Dodson M, Castro-Portuguez R, Zhang DD. NRF2 plays a critical role in mitigating lipid peroxidation and ferroptosis. *REDOX BIOL* 2019;23:101107. 2019-05-01.
- [42] Patinen T, Adinolfi S, Cortes CC, Harkonen J, Jawahar DA, Levonen AL. Regulation of stress signaling pathways by protein lipoxidation. *REDOX BIOL* 2019;23:101114. 2019-05-01.
- [43] Qiu Y, Cao Y, Cao W, Jia Y, Lu N. The application of ferroptosis in diseases. *Pharmacol Res* 2020;159:104919. 2020-05-25.
- [44] Abdalkader M, Lampinen R, Kanninen KM, Malm TM, Liddell JR. Targeting Nrf2 to suppress ferroptosis and mitochondrial dysfunction in neurodegeneration. *Front Neurosci* 2018;12:466. 2018-01-20.